

Does femtosecond time-resolved second-harmonic generation probe electron temperatures at surfaces?

J. Hohlfeld, U. Conrad, and E. Matthias

Fachbereich Physik, Freie Universität Berlin, Arnimallee 14, 14195 Berlin, Germany

Abstract Femtosecond pump-probe second-harmonic generation (SHG) and transient linear reflectivity measurements were carried out on polycrystalline Cu, Ag and Au in air to analyze whether the electron temperature affects Fresnel factors or nonlinear susceptibilities, or both. Sensitivity to electron temperatures was attained by using photon energies near the interband transition threshold. We find that the nonlinear susceptibility carries the electron temperature dependence in case of Ag and Au, while for Cu the dependence is in the Fresnel factors. This contrasting behavior emphasizes that SHG is not *a priori* sensitive to electron dynamics at surfaces or interfaces, notwithstanding its cause.

PACS: 42.65.Ky, 78.47.+p, 63.20.Kr

Nonlinear optical techniques like second-harmonic and sum-frequency generation gain increasing importance for the investigation of surfaces [1], interfaces [2], thin films [3], and multilayers [4]. This trend is intensified by the possibility to investigate the electron dynamics with femtosecond time resolution. For example, Hicks *et al.* [5] used second-harmonic generation on Ag(110) surfaces to study the time dependence of lattice temperature after pulsed laser excitation, and ultrafast laser-induced order/disorder transitions were detected by pump-probe SHG in semiconductors [6, 7, 8]. A broader application of these ultrafast techniques to surface and thin film physics is expected, but increased use of time-resolved SHG requires a more detailed understanding of the influence of transient electron temperatures on the nonlinear signal [5, 9].

The SHG yield is determined by the linear optical properties of the material for the fundamental and frequency-doubled radiation, given by the Fresnel factors $f(\omega)$ and $F(2\omega)$, and its intrinsic ability to generate the second harmonic, characterized by the nonlinear susceptibility, $\chi^{(2)}$ [10]. All three quantities may

be affected by the electron temperature. While $f(\omega)$ and $F(2\omega)$ sample the material within their optical penetration depth, $\chi^{(2)}$ is surface sensitive within the dipole approximation for centrosymmetric materials. Hence, in order to uncover possible differences in electron dynamics of bulk material, surfaces, and thin films, it is of importance to isolate the temperature dependence of each individual factor.

In this contribution, femtosecond time-resolved SHG in combination with transient linear reflection at frequencies ω and 2ω was utilized to study the temperature dependence of $\chi^{(2)}$ for polycrystalline Cu, Ag, and Au samples. It is demonstrated that pump-probe SHG is particularly sensitive to transient electron temperatures when photon energies near interband transitions are used. The 2eV photon energy of the laser employed nearly matches the energy difference between d-band and Fermi energy for Cu and Au [11, 12], while in case of Ag this separation is about 3.9eV [13] and thus almost resonant with $2\hbar\omega$. Broadening and shifting of the Fermi distribution due to absorption leads to changes in electronic occupancy which sensitively affects both the dielectric function [9, 12] and the nonlinear susceptibility [14]. The influence of lattice temperature increase on optical properties is negligible for our experimental conditions [11].

1 Experimental details

The experimental setup was reported in detail in [9]. Laser pulses of 100 fs duration at a wavelength of 630 nm (2 eV) were generated by a colliding-pulse mode locked dye laser and amplified to 50 μJ at repetition rates of a few Hz. For all SHG measurements, identical pump and probe pulses of energies between 12 and 16 μJ and foci of 0.2 mm were used, and the change of the probe pulse SHG yield due to the pump pulse was recorded. The choice of identical pump and probe pulse energies caused strong heating due to the probe pulse, but was necessary to obtain detectable SHG yield. The effective area monitored by SHG corresponded to about one half of the beam area and was therefore nearly homogeneously heated. Great care was taken to work at intensities that caused no surface damage. Probe pulses were delayed with respect to pump pulses by a computer controlled delay stage with 0.1 μm accuracy and a typical step size of 3 μm . In all measurements reported here we used p-polarized fundamental and second harmonic light. To correct for a varying laser intensity, a reference signal was used to record only signals within an intensity interval of $\pm 5\%$. Measurements of the linear reflectivity $R(\omega)$ were carried out with pump and probe pulses focused to about 0.5 mm and 0.2 mm, respectively. Frequency-doubled probe pulses were used to obtain $R(2\omega)$. For linear reflectivity measurements the probe pulses were attenuated by a factor of 5×10^3 . The measurements were carried out under normal conditions at incident angles of 43° (pump) and 48° (probe). All data points in Figs. 1-4 correspond to an average over about

500 shots, and represent relative changes of probe beam signals normalized to values at negative delays.

2 Data analysis

Information about the electron temperature dependence of $\chi^{(2)}$ from time-resolved SHG measurements on polycrystalline metals requires knowledge about (i) the magnitude of the three independent tensor elements of $\chi^{(2)}$ and possible nonlocal contributions, (ii) the variation of $\epsilon(\omega)$ and $\epsilon(2\omega)$ with electron temperature T_e , and (iii) the electron temperature relaxation.

To obtain the electron temperature dependence of $\epsilon(\omega)$ and $\epsilon(2\omega)$ and the time dependence of T_e , we analyzed time-resolved measurements of linear reflectivities at photon energies of fundamental (2 eV) and frequency-doubled light (4 eV). As an example, results of transient linear reflectivities at 2 eV for Au (dots) of a 2.5 μm (bulk) sample and a 20 nm thin film, for which electron diffusion is negligible, are compared to corresponding model calculations (solid lines) in Fig. 1. Although the ratio of the pump intensities used for the thin film and the 2.5 μm sample was only 1.2 : 1, the transient change of R for the thin film is more than twice as large as that for thick metal. The considerably longer relaxation time for the thin film also signals reduced electron cooling and confirms the importance of diffusive heat transport by electrons in bulk metals.

The model calculations are based on knowledge of the dielectric functions, $\epsilon(\omega)$ and $\epsilon(2\omega)$, and of the electron temperature, T_e . The calculational procedure followed here was described in [9] and is as follows: (1) Tabulated experimental values of $\epsilon(\omega)$ [15] were fitted to the model of Rustagi [16] to derive the functional dependence of ϵ on photon energy in the range 1 – 5 eV at room temperature. For the calculation of the dielectric functions the approximation of electron momentum independent transition matrix elements was used [17]. (2) In the same model the electron temperature T_e is contained in the Fermi-function. This allows to calculate $\epsilon(T_e)$ for both photon frequencies ω and 2ω without any additional fit parameters. (3) Cooling of the electron temperature with time was treated according to the two-temperature model by Anisimov *et al.* [18]. The use of the two-temperature model is justified by electron thermalization times of less than 50 fs, predicted for our experimental conditions by the Fermi-liquid theory [19]. In this way we obtained the time-dependence of $\epsilon(\omega)$ and $\epsilon(2\omega)$, fitted to the data in Fig. 1.

No dependence of R on pump-probe delay was found for Ag at 2 eV and for Au at 4 eV, while Cu showed a similar effect at both photon energies. Model calculations lead to good agreement with transient reflectivity data for all three metals.

The variation of $\epsilon(\omega)$ and $\epsilon(2\omega)$ with T_e is now used to predict the effect of transient electron temperatures on the Fresnel factors in SHG. Any deviation from experimental data is then interpreted as electron temperature dependence

of the nonlinear susceptibility. Generally, this is complicated by three independent tensor elements of $\chi^{(2)}$ as well as possible nonlocal contributions. For isotropic bulk material, realized in polycrystalline metals, the *nonlocal response* generates only P-polarized SHG. The corresponding field can be written in the form (Eq. (22) in [10]):

$$E_P^{nl}(2\omega) \propto \gamma \cdot [E_s^2(\omega) + E_p^2(\omega)] . \quad (1)$$

Dipole-allowed surface contributions, on the other hand, are given by Eq. (30) in [10]:

$$E_S(2\omega) \propto \chi_{xxx} \cdot E_s(\omega)E_p(\omega) , \quad (2)$$

$$E_P(2\omega) \propto A \cdot \chi_{xxx} \cdot E_s^2(\omega) + [B \cdot \chi_{zzz} + C \cdot \chi_{xxz} + D \cdot \chi_{zxx}] \cdot E_p^2(\omega) . \quad (3)$$

The different contributions can be separated by polarization dependent measurements.

When analyzing the SH polarization for different polarizations of the fundamental, only P-polarized SHG was detectable for all three metals. It varied with $\cos^4 \Phi$, where Φ is the polarization angle of the incident radiation. Since no S-polarized SH radiation was detectable for arbitrary input polarization, we conclude that χ_{xxx} is vanishingly small. As discussed by Petrocelli *et al.* [20] it is reasonable to assume $\chi_{xxx} \approx \chi_{zxx}$ for polycrystalline metal surfaces. Hence, χ_{zxx} is also small and γ remains the only possible source of P-polarized SH generated by s-polarized input fields. Since no SHG yield was detected for this s-P polarization combination, γ is concluded to be negligible. Summarizing this discussion, the dipole allowed χ_{zzz} connected to the near surface region where symmetry is broken is the only source of SHG.

The second harmonic amplitude can now be expressed in the form [10]:

$$E(2\omega, T_e) \propto F(2\omega) \cdot \chi_{zzz} \cdot f(\omega) \cdot |E(\omega)|^2 = \mathcal{T}_p(T_e) \epsilon(2\omega, T_e) \mathcal{F}_s(T_e) \cdot \chi_{zzz} \cdot f_s^2(T_e) t_p^2(T_e) \cdot |E(\omega)|^2, \quad (4)$$

with

$$f_s(T_e) = \frac{\sin \Theta}{\sqrt{\epsilon(\omega, T_e)}} , \quad f_c(T_e) = \sqrt{1 - f_s(T_e)^2} , \\ t_p(T_e) = \frac{2 \cos \Theta}{\sqrt{\epsilon(\omega, T_e)} \cos \Theta + f_c(T_e)} , \quad (5)$$

where Θ is the angle of incidence. Equivalent expressions for \mathcal{F}_s , \mathcal{F}_c , and \mathcal{T}_p with $\epsilon(2\omega, T_e)$ are used, with lower case (capital) letters denoting quantities of the fundamental (second harmonic) radiation.

The relative change of $|\chi_{zzz}|^2$ with T_e can be extracted from the differences $\Delta SH = SH(T_e) - SH_0$ of measured (SH_m) and predicted (SH_p) second-harmonic intensities:

$$\frac{\Delta|\chi_{zzz}|^2}{|\chi_{zzz}|^2} = \frac{\Delta SH_m - \Delta SH_p}{SH_p(T_e)}, \quad (6)$$

where SH_0 is the yield for the probe pulse alone.

3 Second-harmonic reflectivities

Results of pump-probe SHG measurements are shown in Fig. 2 for Cu and Ag, and in Fig. 3 for Au. Plotted are the relative changes of the probe SHG signal as a function of delay between pump and probe pulses. The peaks around zero delay correspond to a coherent artifact between pump and probe beams and will not be discussed here. Predictions based on Eq. (4), with constant $\chi^{(2)}$ and the temperature dependence exclusively in the Fresnel factors, are indicated by dotted lines. Solid lines represent smoothed relative changes of $|\chi_{zzz}|^2$ with electron temperature, determined by Eq. (6).

For Cu, the dielectric functions describe the temperature dependence of the SHG data well, and we conclude that $\chi^{(2)}$ is in first order independent of electron temperature in the intensity range used. In contrast, for Ag and Au the temperature dependence of SHG is almost entirely contained in the nonlinear susceptibility.

Another way of presenting the data derived from Eq. 6 is shown in Fig. 4, where the relative change of $|\chi_{zzz}|^2$ is plotted versus electron temperature.

For this, we used the correlation between electron temperature and time scale given by the analysis of the linear reflectivities (Fig. 1). From Fig. 4 it is obvious that for Cu χ_{zzz} does not depend on temperature. For Ag and Au, $\Delta|\chi_{zzz}|^2$ depends linearly on T_e . The different signs of the slopes reflect the mismatch between the photon energy at ω (Au) and 2ω (Ag) and the interband transition thresholds. Although no theoretical prediction about the temperature dependence of $|\chi_{zzz}|^2$ is reported in the literature, it is reasonable to assume that $|\chi_{zzz}|^2$, like the linear reflectivity, depends linearly on small temperature variations. Thus, the linear dependencies of $|\chi_{zzz}|^2$ on T_e for Ag and Au indicate similar electron dynamics at the surface and in the bulk. Deviations for Au above 5500 K may actually originate from different electron dynamics at the surface and in the bulk during the first 200 fs but may also reflect a nonlinear temperature dependence of $|\chi_{zzz}|^2$.

Regarding surface contaminations, no evidence for it was found for Ag and Au. On copper surfaces an oxide layer reduces the total SHG yield [22, 23] and may in fact cause that $|\chi_{zzz}|^2$ is independent of electron temperature. Therefore, the measurements on copper should be repeated under UHV-conditions. Nevertheless, the influence of the oxide layer on the electron temperature dependence

of the Fresnel factors remains small, as determined by the time dependence of the linear reflectivity. Thus, notwithstanding whether or not $\chi^{(2)}$ is influenced by the copper oxide/copper interface, we have demonstrated that there are systems like Au and Ag, where time resolved SHG monitors the electron temperature relaxation at the surface, and others, like Cu in air, where SHG is only sensitive to the electron temperature in the bulk.

4 Conclusion

Femtosecond time-resolved SHG with photon energies near the interband transition threshold was demonstrated to be a powerful tool for investigating electron dynamics in noble metals. Transient linear reflectivities were combined with pump-probe SHG data to separate the dependence of Fresnel factors and $\chi^{(2)}$ on electron temperature. A contrasting behavior was found. In case of Cu, transient electron temperatures affect the Fresnel factors, $\chi^{(2)}$ is independent of electron temperature, and there is no surface sensitivity. For Ag and Au, $\chi^{(2)}$ varies with electron temperature and pump-probe SHG monitors the electron relaxation near the surface.

Acknowledgements. This work was supported by the Deutsche Forschungsgemeinschaft, Sonderforschungsbereich 290. The experiments were performed at the Laboratory for Applications of the Max-Born-Institut Berlin, and the cooperation of Dr. F. Noack and his team is gratefully acknowledged. We also thank Dr. W. Hübner for fruitful discussions.

References

- [1] Y.R. Shen, Appl. Phys. **A** 59, 541 (1994), Surf. Sci. 299/300, 551 (1994).
- [2] G.L. Richmond, J.M. Robinson, and V.L. Shannon, Progr. Surf. Sci. 28, 1 (1988).
- [3] F.R. Aussenegg, A. Leitner, and H. Gold, Appl. Phys. **A** 60, 97 (1995).
- [4] T. Rasing, Appl. Phys. **A** 59, 531 (1994).
- [5] J.M. Hicks, L. E. Urbach, E. W. Plummer, and Hai-Lung Dai, Phys. Rev. Lett. 61, 2588 (1988).
- [6] H.W.K. Tom, G.D. Aumiller, and C.H. Brito-Cruz, Phys. Rev. Lett. 60, 1438 (1988).
- [7] P. Saeta, J. - K. Wang, Y. Siegal, N. Bloembergen, and E. Mazur, Phys. Rev. Lett. 67, 1023 (1991).

- [8] K. Sokolowski-Tinten, J. Bialkowski, and D. von der Linde, Phys. Rev. **B** 51, 14186 (1995).
- [9] J. Hohlfeld, U. Conrad, D. Grosenick, and E. Matthias, Appl. Phys. **A** 60, 137 (1995).
- [10] J.E. Sipe, D.J. Moss, and H.M. van Driel, Phys. Rev. **B** 35, 1129 (1987).
- [11] G.L. Eesley, Phys. Rev. Lett. 51, 2140 (1983).
- [12] R.W. Schoenlein, W. Z. Lin, and J. G. Fujimoto, and G. L. Eesley, Phys. Rev. Lett. 58, 1680 (1987).
- [13] N.E. Christensen, phys. stat. sol. (b) 54, 551 (1972).
- [14] O. Keller, Phys. Rev. **B** 33, 990 (1986).
- [15] E. D. Palik, editor, Handbook of optical constants of solids (1985).
- [16] K. C. Rustagi, Il nuovo cimento **LIII**, 346 (1968).
- [17] C.-K. Sun, F. Vallée, L. H. Acioli, E. P. Ippen, and J. G. Fujimoto, Phys. Rev. **B** 50, 15337 (1994).
- [18] S.I. Anisimov, B.L. Kapeliovich, and T.L. Perel'man, Sov. Phys. JETP 39, 375 (1975).
- [19] D. Pines and P. Nozières, *The Theory of Quantum Liquids* (Benjamin Press, New York, 1966).
- [20] G. Petrocelli, S. Martellucci, and R. Francini, Appl. Phys. **A** 56, 263 (1993).
- [21] C.M. Li, L.E. Urbach, and H.L. Dai, Phys. Rev. **B** 49, 2104 (1994).
- [22] J. Bloch, D. J. Bottomley, S. Janz, and H. M. van Driel, Surf. Sci. 257, 328 (1991).
- [23] H.W.K. Tom, and G. D. Aumiller, Phys. Rev. **B** 33, 8818 (1986).

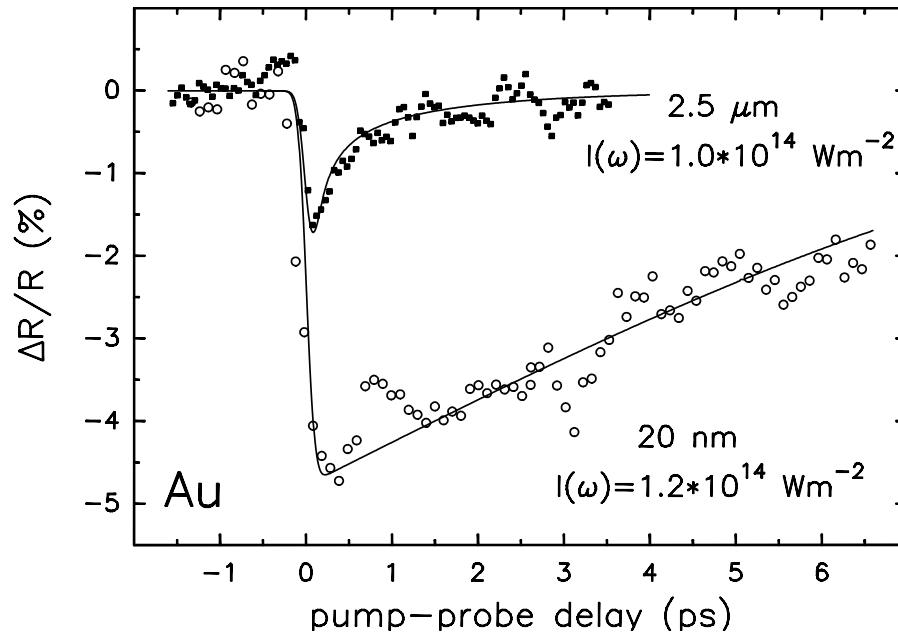


Figure 1: Relative change of transient linear reflectivities at a photon energy of 2 eV for 2.5 μm (bulk) and 20 nm thick samples of Au. Solid lines represent model calculations with the same electron-phonon coupling in both cases. Electron diffusion was taken into account for the 2.5 μm sample but neglected for the 20 nm film.

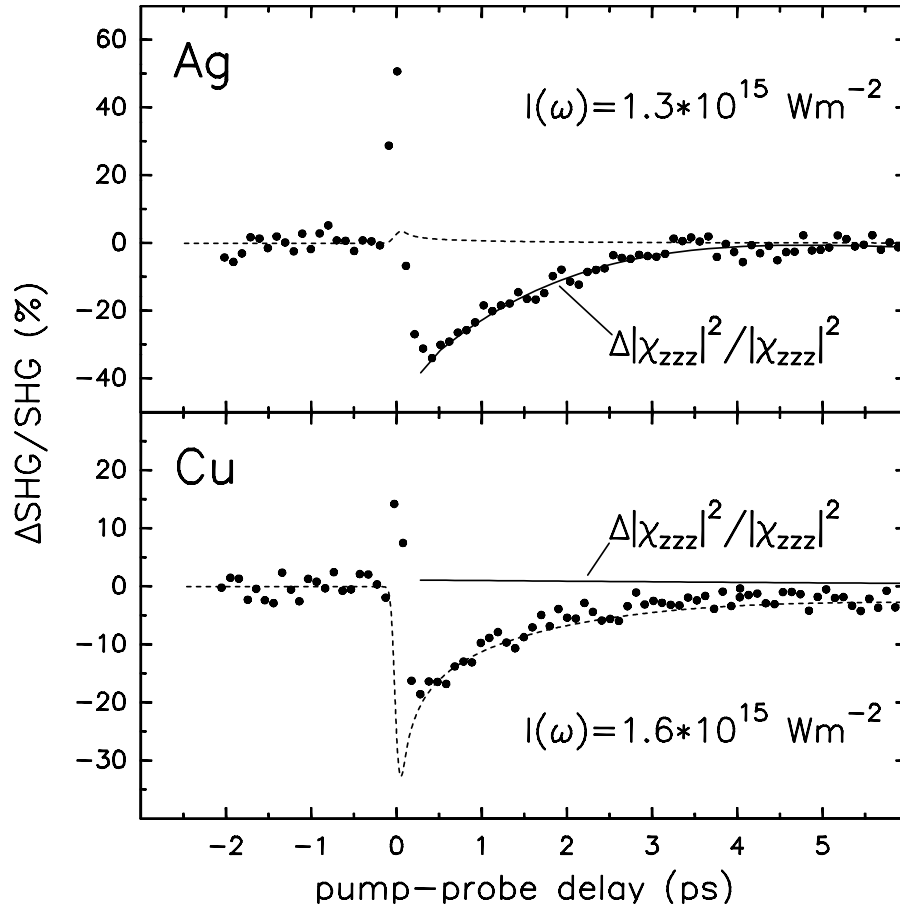


Figure 2: Relative changes of SHG yield (dots) versus pump-probe delay time for Ag and Cu. The data are normalized to the SHG yield of the probe pulses at negative delays. Dotted lines indicate the electron temperature dependence of SHG due to the Fresnel factors only. Solid lines originate from the difference between smoothed experimental data and dotted lines and represent the relative change of $|\chi_{zzz}|^2$ with electron temperature.

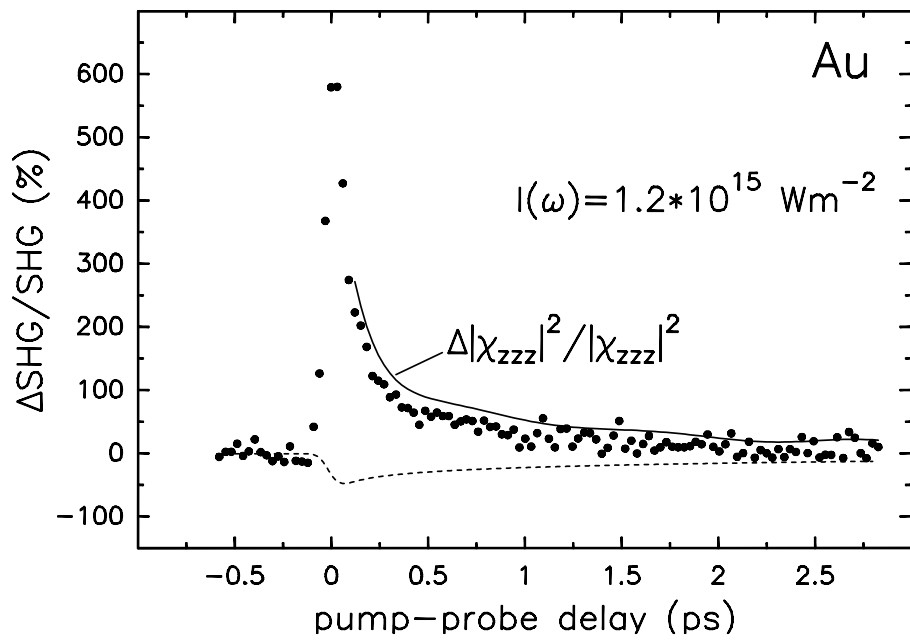


Figure 3: Relative changes of SHG yield (dots) versus pump-probe delay time for the $2.5 \mu\text{m}$ Au sample. Description of solid and dotted lines as in Fig. 3.

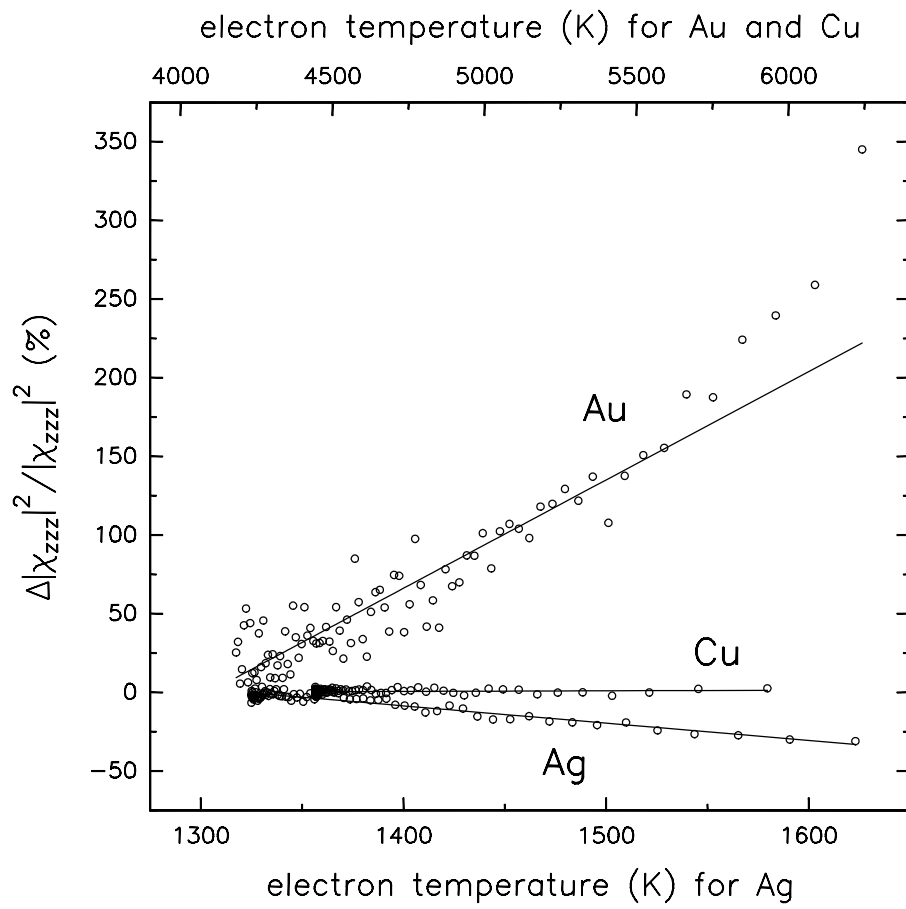


Figure 4: Relative changes of $|\chi_{zzz}|^2$ with electron temperature for Cu, Ag, and Au.